Available online at www.sciencedirect.com
ScienceDirect
Thermochimica Acta 455 (2007) 50–54
thermochimica acta
www.elsevier.com/locate/tca

Interfacial effect on thermal conductivity of Y_2O_3 thin films deposited on Al_2O_3

Ho-Soon Yang [a], J.W. Kim [b], G.H. Park [a], C.S. Kim [a], K. Kyhm [c], S.R. Kim [d], K.C. Kim [b], K.S. Hong [e,*]

[a] *Department of Physics, Pusan National University, Pusan 609-735, Republic of Korea*
[b] *Department of Mechanical Engineering, Pusan National University, Pusan 609-735, Republic of Korea*
[c] *Research Center for Dielectric and Advanced Matter Physics, Pusan National University, Pusan 609-735, Republic of Korea*
[d] *LG Electronics, Changwon 641-711, Republic of Korea*
[e] *Pusan Center, Korea Basic Science Institute, Pusan 609-735, Republic of Korea*

Abstract

The interfacial effect on thermal conductivity is studied with Y_2O_3 thin films deposited on an Al_2O_3 substrate. Y_2O_3 thin films with the thickness between 100 and 500 nm are prepared using rf magnetron sputtering and thermal conductivity of the films is measured using the 3ω method. The strong film thickness-dependent thermal conductivity due to the interfacial thermal resistance is observed. The film thickness-dependent thermal conductivity is explained by an interface thermal resistance between the film and substrate.

Keywords: Interfacial thermal resistance; 3ω method; Yttrium oxide; Aluminum oxide; Thermal conductivity; rf magnetron sputtering

1. Introduction

Yttrium oxide (Y_2O_3) is a suitable material for a metal/insulator/semiconductor structure due to its particular physical properties such as a high dielectric constant (12–18), a wide band gap energy (5.5 eV), and high thermal stability up to 2300 °C [1]. The interfacial effect becomes more important in determining the physical properties as the system size decreases [2]. There have been reports on the reduced thermal conductivity of dielectric material consisting of nano-sized grains and films [3–5]. Nanocrystalline yttria-stabilized zirconia (YSZ) showed the strongly grain size-dependent thermal conductivity at temperatures between 6 and 480 K and the interfacial thermal resistance of grain boundaries was determined with the measured grain size-dependent thermal conductivity of YSZ [3]. Yamane et al. [4] reported the film thickness-dependent thermal conductivity of SiO_2 thin films deposited on Si and obtained the interfacial thermal resistance of SiO_2/Si from the film thickness-dependent thermal conductivity. As the technology to produce miniature devices has developed rapidly, the interfacial effect becomes more important. While Y_2O_3 has been considered as a suitable material for a metal/insulator/semiconductor structure, no much work about the interfacial effect on thermal conductivity of Y_2O_3 thin films has been performed. This work focuses on the interfacial effect on thermal conductivity of thin films.

In this study, the interfacial effect on thermal conductivity is studied with Y_2O_3 thin films deposited on Al_2O_3 substrates. Y_2O_3 thin films with thickness between 100 and 500 nm are prepared on Al_2O_3 substrates using rf magnetron sputtering. The optimized conditions for the growth of Y_2O_3 thin films are determined as varying the rf power, substrate temperature, post-annealing temperature, and deposition time. Thermal conductivity of Y_2O_3 films was measured using the 3ω method and the film thickness-dependent thermal conductivity is understood with the interfacial thermal resistance.

2. Experimental details

Y_2O_3 films are deposited on Al_2O_3 substrates using rf magnetron sputtering. The source material is a Y_2O_3 ceramic target of 2 in. diameter and 0.25 in. thickness with 99.99% purity. During the deposition, the substrate is heated and rotated with 3 rpm for the uniform film growth. Y_2O_3 films are grown as varying the rf power, substrate temperature, gas pressure, post-annealing

---

[*] Corresponding author. Tel.: +82 51 510 2991; fax: +82 51 517 2497.
E-mail address: kyongsoo@kbsi.re.kr (K.S. Hong).

0040-6031/$ – see front matter © 2007 Elsevier B.V. All rights reserved.
doi:10.1016/j.tca.2006.11.030

Table 1
Sputtering conditions for the growth of Y_2O_3 thin films

Substrate	Al_2O_3
Target	Y_2O_3 ceramic target
Substrate–target distance	8 cm
Sputtering gas	Ar (99.999 %), O_2 (99.99 %)
Base pressure	5×10^{-6} Torr
Working pressure	3×10^{-2} Torr
Substrate temperature	600 °C
rf power	160 W
Post-annealing	800 °C for 2 h
Deposition time	25–150 min

temperature, and deposition time. The film structures are analyzed with an X-ray diffraction (XRD: Rigaku GDX-11P3A) patterns obtained with Cu Kα radiation ($\lambda = 0.15406$ nm). Scanning electron microscopy (SEM: Hitachi S-4200) is used to confirm the film surface and thickness. The best growing conditions are determined with the crystal structure and surface roughness of films. Table 1 shows the sputtering conditions for Y_2O_3 thin films. The deposition rate is obtained from the relationship between deposition time and film thickness, and then the thickness of Y_2O_3 films is controlled between 100 and 500 nm as varying the deposition time.

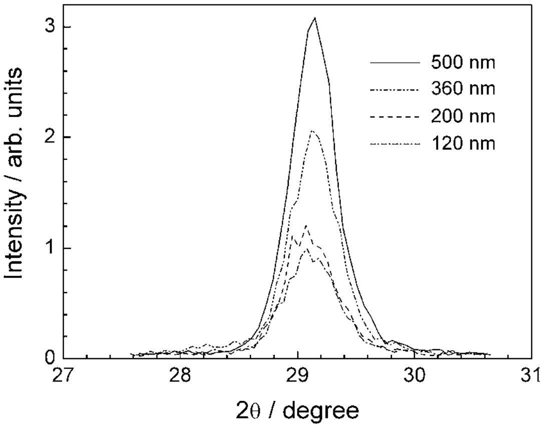

Fig. 2. XRD patterns of Y_2O_3 films with 120, 200, 360, and 500 nm thicknesses.

Table 2
X-ray diffraction peak positions and FWHM obtained from the XRD patterns of Y_2O_3 films shown in Fig. 2

Film thickness (nm)	Peak position (°)	FWHM (°)
120	29.083	0.437
200	29.075	0.427
360	29.123	0.399
500	29.130	0.386

Thermal conductivity of Y_2O_3 (=14.2 W m^{-1} K^{-1}) thin films is measured using the 3ω method. Gold is used for the metal line which serves as both heater and thermometer, and chromium is used for an intermediate layer to improve the adhesion of gold. Gold and chromium are deposited on a sample by electron beam evaporation and a metal line is patterned with photolithography and etching process. ac current of frequency ω is driven to the metal line, which results in generating heat of frequency 2ω. Since the resistance of the metal line increases linearly as the temperature increases, the frequency-dependent temperature oscillation of the metal line is obtained from the voltage oscillation at frequency 3ω measured with a lock-in amplifier (SR850). The experimental details of the 3ω method are well described elsewhere [4,5]. Measurements of the thermal conductivity of Y_2O_3 thin films with thickness 120, 200, 360 and 500 nm are performed three times at room temperature. We measure the electrical resistance, R, of a metal line on each film at four different temperatures. dR/dT of metal lines on 120, 200, 360 and 500 nm films is 0.02063, 0.01879, 0.02262, and 0.01736 Ω/°C, respectively, with which the temperature of metal lines are calibrated.

3. Results and discussion

It is found from the measurement of the film thickness with SEM that the film thickness increases linearly with a deposition time, which gives the deposition rate, 3.05 nm/min. The film thickness can be controlled as varying the deposition time. Fig. 1 shows the cross-sectional and surface SEM images of a 360 nm thick Y_2O_3 films after post-annealing at 800 °C for 2 h.

Fig. 2 shows the XRD patterns of 120, 200, 360, and 500 nm thick Y_2O_3 films grown for 25, 50, 100, and 150 min, respectively. The main XRD peak at 29.15° corresponds to the (2 2 2) reflections in bulk Y_2O_3 crystals [6]. Table 2 presents the main peak positions and the full widths at half maximum (FWHM) of the Y_2O_3 films from the analysis of XRD results. The main

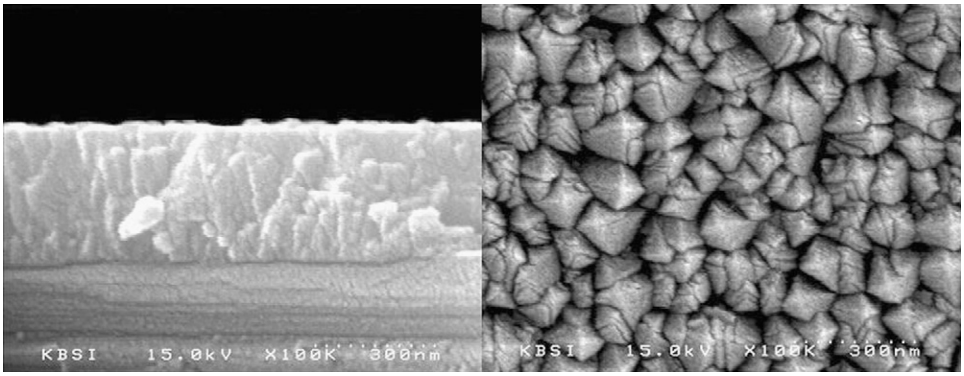

Fig. 1. SEM images of cross-sectional and surface views of a 360 nm thick Y_2O_3 film after post-annealing at 800 °C for 2 h.

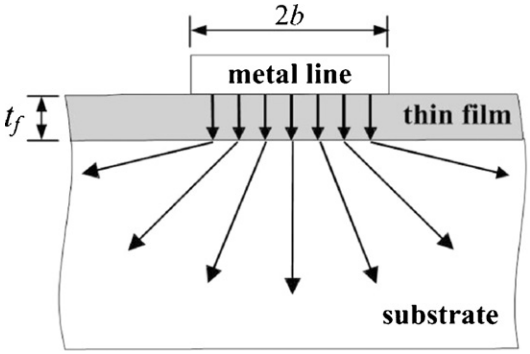

Fig. 3. Schematic diagram of heat flow through thin film and substrate in 3ω measurement. Heat is represented with arrows. t_{f} and 2b are film thickness and metal line width, respectively.

peak positions of thin films shift close to 29.15° and FWHM of the peak decreases as the film thickness increases. This result indicates that the lattice constant of Y_2O_3 films is larger than that of bulk Y_2O_3 due to the strain of the lattice-mismatched substrate which becomes weaker as the film becomes thicker.

Fig. 3 shows schematically the heat flow through thin film and substrate in the 3ω method. The thermal conductivity of thin film is smaller than that of substrate. Fourier's law explains the one-dimensional heat flow in the film where the film thickness is smaller than the thermal penetration depth of film. The heat flow in the substrate is frequency-dependent radial flow, where the substrate thickness is much larger than the thermal penetration depth in the substrate. The temperature oscillation of the metal line is represented with the temperature oscillations of the substrate, ΔT_{s}, and thin film, ΔT_{f} [4,5]:

$$\Delta T(\omega) = \Delta T_{\mathrm{s}}(\omega) + \Delta T_{\mathrm{f}} = \frac{P}{l\pi k_{\mathrm{s}}}\int_0^{\infty}\frac{\sin^2(\lambda b)}{(\lambda b)^2(\lambda^2+q^2)^{1/2}}\,\mathrm{d}\lambda + \frac{Pt_{\mathrm{f}}}{2lbk_{\mathrm{f}}} \qquad (1)$$

where P is the power, l and b the length and half-width of the heater, respectively, q the complex thermal wave number, t_{f} the film thickness, and k_{s} and k_{f} are thermal conductivity of the substrate and the film, respectively. If $|q|b < 1$, the temperature oscillation of metal line is approximated as

$$\Delta T(\omega) = \frac{P}{\pi l k_{\mathrm{s}}}\left(\frac{1}{2}\ln\frac{D_{\mathrm{s}}}{b^2} + \eta - \frac{1}{2}\ln(2\omega) - \frac{\mathrm{i}\pi}{4}\right) + \frac{Pt_{\mathrm{f}}}{2lbk_{\mathrm{f}}} \qquad (2)$$

where D_{s} is the thermal diffusivity of the substrate and ω is a frequency of the driven current [4,5].

Thermal conductivity of the substrate can be obtained from the amplitude of temperature oscillation of the metal line as a function of frequency. Fig. 4 shows the measured amplitude of the temperature oscillation of the heater on a bare Al_2O_3 substrate. The length, l, and width, 2b, of the heater are 3.123 mm and 29.268 μm, respectively. The in-phase amplitude represented by the closed squares shows a good agreement with the calculated in-phase amplitude of the temperature oscillation given by Eq. (2). The thermal conductivity of Al_2O_3, 35.82 W m^{-1} K^{-1}, is determined from the slope of the in-phase temperature amplitude of the metal line as a function of logarithmic frequency.

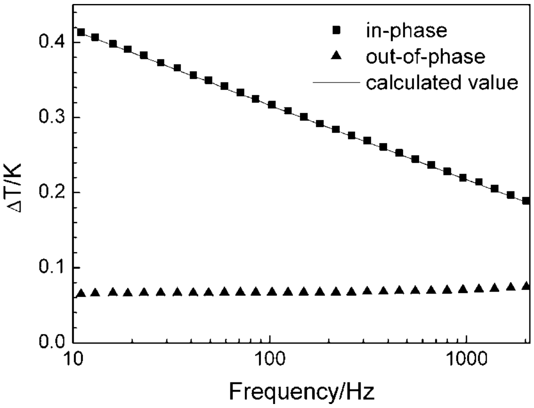

Fig. 4. The amplitude of the temperature oscillation of a heater on a bare Al_2O_3 substrate as a function of the frequency of a driven current. The closed squares (■) and closed triangles (▲) represent the measured in-phase and out-of-phase amplitudes of the temperature oscillation, respectively. The solid line represents the calculated in-phase amplitude.

The temperature oscillation of thin film which is frequency-independent, the second term in Eq. (2), is the difference between the measured temperature oscillation of metal line and the temperature oscillation of the substrate. Thermal conductivity of the film can be determined by

$$k_{\mathrm{f}} = \frac{P}{l\Delta T_{\mathrm{f}}}\frac{t_{\mathrm{f}}}{2b} \qquad (3)$$

Fig. 5 shows the amplitude of temperature oscillation of the heater (l = 3.123 mm and 2b = 29.268 μm) on a 360 nm thick Y_2O_3 film deposited on the Al_2O_3 substrate. The temperature oscillation of the substrate is shown with a solid line. The amplitude of the temperature oscillation in the presence of Y_2O_3 film on substrate increases compared with that of a bare substrate. The increment of amplitude due to the thin film is independent of the frequency of the driven current. The

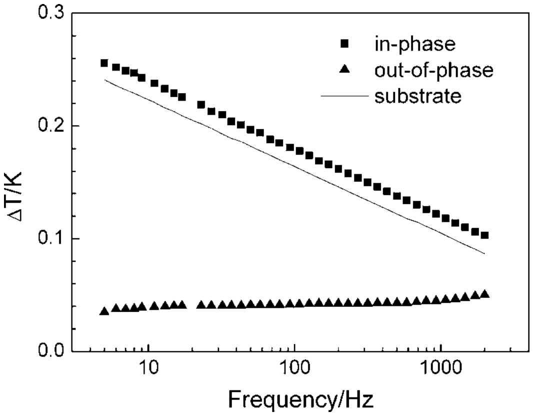

Fig. 5. The amplitude of the temperature oscillation of a heater on a 360 nm thick Y_2O_3 film as a function of frequency of driven current. The closed squares (■) and closed triangles (▲) represent the measured in-phase and out-of-phase amplitudes of temperature oscillation, respectively. The solid line represents the calculated in-phase amplitude of temperature oscillation in the Al_2O_3 substrate.

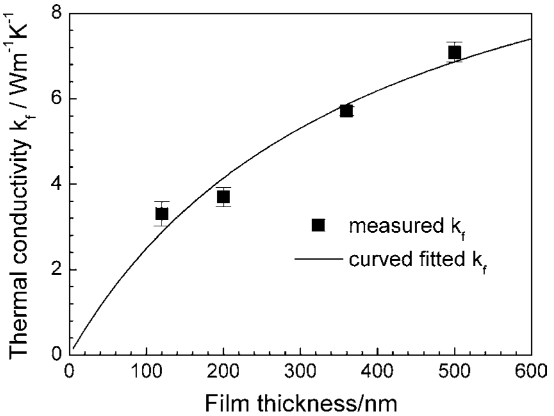

Fig. 6. The measured thermal conductivity of Y_2O_3 films on Al_2O_3 substrates as a function of film thickness. The measured thermal conductivity of Y_2O_3 films is represented by the closed squares (■). The solid line is a fit of the result by Eq. (4).

thermal conductivity of 360 nm thick Y_2O_3 film at room temperature, 5.8334 W m^{-1} K^{-1}, is calculated from Eq. (3). Thermal conductivities of 120, 200 and 500 nm thick Y_2O_3 films are also obtained as following the same procedures and the film-thickness dependence of thermal conductivity is shown in Fig. 6. Y_2O_3 thin films exhibit substantially reduced thermal conductivity compared with single crystal Y_2O_3 due to the interfacial effect.

In order to understand the interfacial effect on thermal conductivity, we can model a temperature profile across a thin film having an interface with a substrate as shown in Fig. 7. It is assumed in this model that the thermal conductivity of a interior region of films is independent of film thickness. Temperature difference across a thin film consists of temperature difference in an interior region of film, T_o, and temperature discontinuity at an interface, T_{gb}. The effective thermal conductivity of thin film can be defined as [3,4,7]

$$k_f = \frac{k_i}{1 + k_i R_k / t_f} \tag{4}$$

where k_i is thermal conductivity of an interior region of film, R_k is an interfacial resistance (the Kapitza resistance), and t_f is a film thickness. The solid line in Fig. 6 is a fit to the experimental data given by Eq. (4). The effective thermal resistance, R_f, of a thin film can be written from Eq. (4) as

$$R_f = \frac{t_f}{k_f} = R_k + \frac{1}{k_i} t_f \tag{5}$$

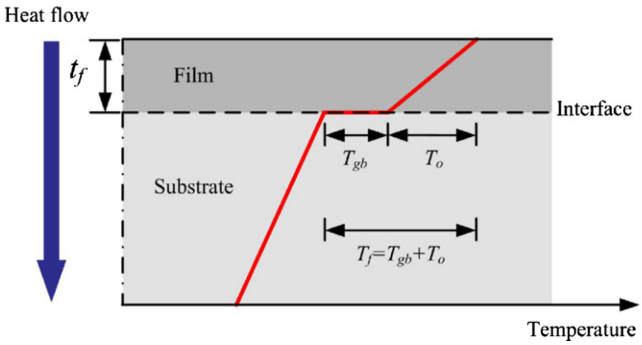

Fig. 7. One-dimensional temperature profile across thin film in response to an applied heat flux. The temperature drop across an interior region of film is denoted by T_o. T_{gb} denotes a temperature discontinuity resulting from the interfacial resistance.

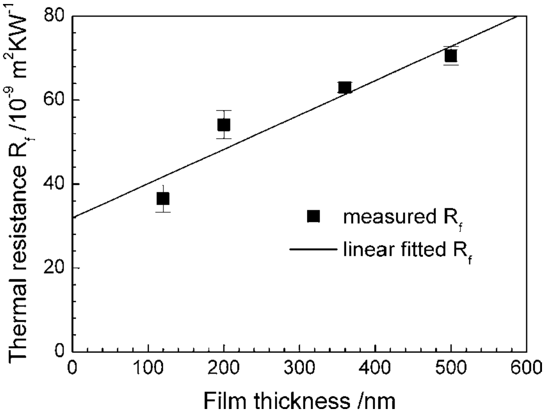

Fig. 8. Thermal resistance of Y_2O_3 films on Al_2O_3 substrate as a function of film thickness denoted by closed squares (■). The result is fitted by Eq. (5) and represented by a solid line.

Fig. 8 shows the effective thermal resistance obtained from the measurement. The closed squares and solid line represent the experimental values and a fit to the data by Eq. (5), respectively and the intercept on a y-axis gives the value of interfacial thermal resistance.

The interfacial thermal resistance between Y_2O_3 and Al_2O_3, $R_k = 3.1954 \times 10^{-8}$ m^2 kW^{-1}, and thermal conductivity of the interior region, $k_i = 12.217$ W m^{-1} K^{-1}, were determined from the fits in Figs. 6 and 8. Thermal conductivity of the interior region is approximately 85% of the intrinsic thermal conductivity of Y_2O_3 from Ref. [8].

There are only a few materials known for the interfacial thermal resistance. Since the interfacial resistance is the order of 10^{-7} to 10^{-8} m^2 kW^{-1}, it has only a small effect on an effective thermal conductivity in bulk systems. As systems become miniature, the interfacial effect should be considered in determining thermal properties of the system.

4. Conclusion

Y_2O_3 films are deposited on Al_2O_3 substrates using rf magnetron sputtering as varying the film thickness between 100 and 500 nm. The film thickness, structures, and surface conditions are analyzed with XRD patterns and SEM images. Thermal conductivity of Y_2O_3 thin films is measured with the 3ω method.

Y_2O_3 thin films on Al_2O_3 substrate exhibit the apparent film thickness-dependent thermal conductivity. As the thickness of Y_2O_3 thin films decreases, thermal conductivity of Y_2O_3 films is reduced due to the interfacial thermal resistance. The intrinsic thermal conductivity of Y_2O_3 thin film and interfacial thermal resistance between Y_2O_3 and Al_2O_3 are determined with the measured thickness-dependent thermal conductivity of Y_2O_3 films.

The interfacial thermal resistance between Y_2O_3 and Al_2O_3 is higher than those reported in other metal oxides, which implicates the potential as thermal barrier materials. It still needs more study about mechanical properties, stability of interfaces, etc. for real applications. Since the interfacial effect varies with the combination of materials, experimental study of the interfacial resistance between various metal oxides needs to be performed.

Acknowledgements

This work was supported by Korean Research Foundation Grant, KRF-2003-015-C00227, and grant No. RTI04-02-01 from the Regional Technology Innovation Program of the Ministry of Commerce, Industry and Energy, Korea.

References

[1] A.C. Rastogi, R.N. Sharma, J. Appl. Phys. 71 (1992) 5041–5052.
[2] R.N. Sharma, S.T. Lakshmikumar, A.C. Rastogi, Thin Solid Films 199 (1992) 1–8.
[3] H.-S. Yang, G.-R. Bai, L.J. Thompson, J.A. Eastman, Acta Materialia 50 (2002) 2309–2317.
[4] T. Yamane, N. Nagai, S.-I. Katayama, M. Todoki, J. Appl. Phys. 91 (2002) 9772–9776.
[5] D.G. Cahill, A. Bullen, S.-M. Lee, High Temperatures-High Pressures 32 (2000) 135–142.
[6] JCPDS File 88-1040, International Committee for Diffraction Data, Powder Diffraction File.
[7] C.-W. Nan, R. Birringer, Phys. Rev. B 57 (1997) 8264–8268.
[8] A.L. Edwards, For Computer Heat-Conduction Calculations—A Compilation of Thermal Properties Data, UCRL-50589, February 24, 1969.